Suspension stability analysis of soil along the metro lines impact by strong vibrations traffic load

LV Xiangfeng[1,2], YANG Dongbo[1], ZHOU Hongyuan[1,2]

[1]Beijing Municipal Engineering Research Institute, Geotechnical Engineering Technology Research Center, Beijing, China.
[2]Beijing Municipal Construction Engineering Quality Third Test Institute, Beijing, China.

*Presenting author: szgcyjylvxiangfeng@163.com
†Corresponding author: 973087860@qq.com

Abstract

Under the action of strong vibration load, the safety threat of deep buried chamber greatly increased, this bring serious challenges to the excavation of deep underground engineering. Therefore, it is urgent to carry out the research on the reinforcement and vibration reduction of deep buried chamber. Based on the continuum mechanics of discrete element method, the vibration reduction and reinforcement of the rigid support and rigid flexible coupling support of deep buried chamber were studied. The calculation results show that the traffic vibration stress wave have a wave effect on the whole metro area, when it act on the metro top, it's distribution will approximate to "horns"; Under the vibration load conditions, the concrete segment as a strong energy storage body can improve the passive support strength, but can also lead to the cracks which is caused by the metro extrusion deformation. After set the concrete energy absorbing layer, the seismic wave which is in the vicinity of the metro bottom and the propagation process have been effectively attenuation, the deformation of the soil around metro also reduced. In addition, increasing the strength of concrete segment can greatly improve metro operation safety.

Key words: Strong vibration transportation load, Soil along the metro lines, Concrete energy-absorbing layer, Shock absorption, Numerical studies

Introduction

Along with the increasing of ground traffic shock load, the influence of the strong vibration traffic load on the soil along the metro line became a technical problem to be solved badly [1-3]. A lot of practice proves that under the complicated geological conditions, the large surrounding rock deformation combined with the influence of ground traffic load let the metro control become more difficulty and even let the metro surrounding rock deformation or broken. Therefore, the further analysis of the influence of strong vibration traffic load on the soil along the metro lines, and the shock absorption stability of metro will provide a new method for the metro operation safety, also have important practical significance.

Domestic and foreign researchers have carried out a lot of research on the ground deformation, which is caused by Underground engineering excavation and traffic load. Qian Qihu have studied the challenges faced by underground projects construction safety and it's corresponding measures. Chen li have investigated the mechanism of deformation body of fill subgrade and the treatment engineering measures. Dahl F et al. studied the classifications of properties influencing the drill ability of rocks based on the test method. However, previous studies generally consider the structural stability of layer based on single factor. In fact, the deformation and damaging process is closely related to the coupling effects of high building, overhead bridges and traffic load, which are still in the infant stage.

Under the strong earthquake conditions, this paper use the GPU acceleration technology and discrete element method of continuous media mechanics to study the soil along the metro line and it's shock absorption stability, in order to play a guiding role in metro long-term safety operation.

Discontinuous deformation theory

The block in the calculation of discontinuous deformation is formed by one or more finite element units, continuous structure is used in the block, and discontinuous structure is used on the block boundary.

Governing equation

The governing equation of the discontinuous deformation calculation theory is the motion equation, the block body is subjected to internal force and external force. Internal force include the force which is caused by the deformation of the block and the damping force, external force include the out boundary force and the force between springs. In mechanics, because of the block body is regarded as a continuous, isotropic linear elastic body, so its mechanical properties are described by the basic differential equations of three-dimensional elastodynamics theory, That is:

Equilibrium equation: $\sigma_{ij,j} + f_i - \rho u_{i,n} - \mu u_i = 0$

Geometric equation: $\varepsilon_{ij} = \frac{1}{2}(u_{i,j} + u_{j,i})$

Physical equation: $\sigma_{ij} = \lambda \delta_{ij} \varepsilon_{kk} + 2G\varepsilon_{ij}$

Boundary condition: $u_i = \overline{u}_i$ (on the displacement boundary of Γ_u), $\sigma_{ij} n_j = T_i$ (On the force boundary of Γ_σ)

In the formula, σ_{ij}, u_i, f_i and T_i respectively represent stress, displacement, volume force and area force; Ω and Γ respectively represent the rock block region and its boundary, $\Gamma=\Gamma_u \cup \Gamma_\sigma$, λ and G are lame constant, ρ and μ respectively represent mass density and damping coefficient, δ_{ij} is Kronecker delta symbol. Based on the elastic variational principle, the governing equation of the calculation is the motion equation of block body:

$$[\boldsymbol{M}]\{\ddot{\boldsymbol{u}}(t)\} + [\boldsymbol{C}]\{\dot{\boldsymbol{u}}(t)\} + [\boldsymbol{K}]\{\boldsymbol{u}(t)\} = \{\boldsymbol{Q}(t)\} \quad (1)$$

In the formula, $\{\dot{u}(t)\}$, $\{u(t)\}$, $\{\ddot{u}(t)\}$ respectively represent acceleration array, speed array, displacement array of all the nodes of block body. $[M]$, $[C]$, $[K]$, $[Q]$ respectively represent mass matrix, damping matrix, stiffness matrix and nodal load array.

The calculation of each time step for solving the governing equations is divided into two parts. The first step is to loop each deformable block body, and complete the corresponding continuous deformation calculation. The Second step is to calculate the force of contact surface. Firstly, from the stiffness matrix and the nodal displacement obtain the elastic force, then, from damping matrix and nodal velocity obtain damping force, finally, combining the direct integral method and external force to solve motion equation. Specific equations are:

Elastic force: $$\begin{bmatrix} K_{1,1} & K_{1,2} & \dots & K_{1,n} \\ K_{2,1} & K_{2,2} & \dots & K_{2,n} \\ \dots & \dots & \dots & \dots \\ K_{\mathrm{n},1} & K_{\mathrm{n},2} & \dots & K_{\mathrm{n},n} \end{bmatrix} \begin{bmatrix} u_1 \\ u_2 \\ \dots \\ u_n \end{bmatrix} = \begin{bmatrix} f_1 \\ f_2 \\ \dots \\ f_n \end{bmatrix} \tag{2}$$

Damping force: $$\begin{bmatrix} C_{1,1} & C_{1,2} & \dots & C_{1,n} \\ C_{2,1} & C_{2,2} & \dots & C_{2,n} \\ \dots & \dots & \dots & \dots \\ C_{\mathrm{n},1} & C_{\mathrm{n},2} & \dots & C_{\mathrm{n},n} \end{bmatrix} \begin{bmatrix} v_1 \\ v_2 \\ \dots \\ v_n \end{bmatrix} = \begin{bmatrix} f_1' \\ f_2' \\ \dots \\ f_n' \end{bmatrix} \tag{3}$$

Combining the direct integral method and external force to solve motion equation:

$$\begin{Bmatrix} a_i = (f_i + f_i' + f_i^{out}) / m_i \\ v_i = v_i^{t-1} + a_i t \\ u_i = u_i^{t-1} + v_i t \end{Bmatrix} \tag{4}$$

As shown in the formula (4), through the resultant force to obtain the acceleration, velocity and displacement of block body nodes. f_i^{out} include the forces of boundary surface and the forces of contact surface, boundary conditions provide boundary force.

Model boundary

Figure 1 show the normal and tangential spring of the interface. F_n^j and F_s^j are normal and tangential forces of springs, K_n^j and K_s^j are normal and tangential stiffness of springs, Δd_n^j and Δd_s^j are normal and tangential displacements of springs.

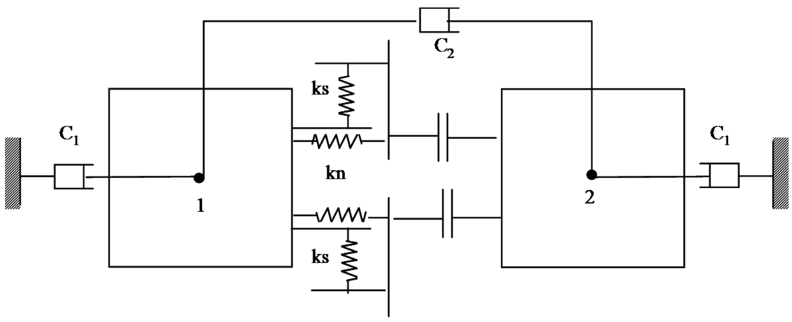

Figure. 1 The normal and tangential spring of the interface

Three dimensional calculation model and parameter selection

The study object is an excavation section of metro engineering, its numerical calculation model size is 24m × 17m × 17m. Circular cross section is adopted to calculate, and its size is ₵ 3m×15m. Elastic plastic model as the calculation model, and the calculation model is divided into four layers，from top to bottom: gravel-boulder bed (5m), roof layer (3m), excavation layer (6m), bottom layer (3m) [4,5]. A total of nine measuring points set on the top plate, the bottom plate and the two sides of model, (The distance between the measuring points is 0.5m. From left to right, the number of the measurement points on both sides of the model are respectively No.1 to No.6.,the bottom plate measuring point is from top to bottom for 7 to 12), row spacing of U-shaped Steel is 2m. The three-dimensional numerical computation model is shown in figure 2. The local geological data is the reference of parameters of the calculation model, and its values are shown in Table 1.

The boundary conditions of model are respectively: bottom surface is full constraint, flank is horizontal constraint, and the top surface is free. Considering the surrounding building load (200-meter- high building, overhead bridges and traffic load), the initial stress of the model boundary as follow: the maximum horizontal stress is 20 MPa, the minimum horizontal stress is 18 MPa, the vertical stress is 17 MPa.

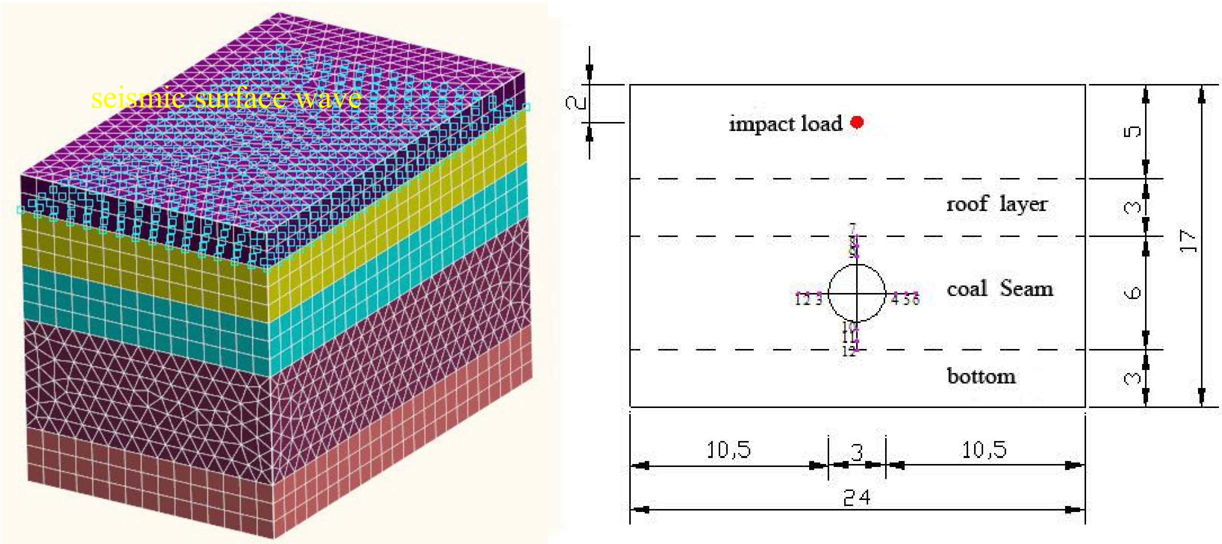

Fig.2 3-D calculation model

Table1 Computing model parameters

Material name	Elastic modulus /E(GPa)	Poisson ratio /μ	Density /ρ (kg/m3)	cohesive strength /C(kPa)	Internal friction angle /φ (°)	Yield strength /(MPa)
Gravel-boulder bed	80	0.25	2300	50	30	42
Roof layer	100	0.2	2440	55	40	60
Excavation layer	3.5	0.28	1700	29	25	20
Bottom layer	90	0.22	2200	52	35	57
Concrete energy absorbing layer	68	0.35	400	—	—	25
Duct piece	210	0.31	7850	—	—	350

Study on the propagation law of the vibration stress wave in soil

Figure 3 shows the calculation results of vertical velocity at different time. From the results we can know that the metro is strong affected by the vibration load. When t=0.5s, the influence of vibration load on metro has enhanced. The vibration load has an upward pushing influence to the floor and both sides of the metro, it also has an downward influence to the metro roof. When t=1s, the vibration influence continue to increase, the influence of vibration load on the metro roof is approximated to the shape of sheep horns, the whole metro have an upward tendency.

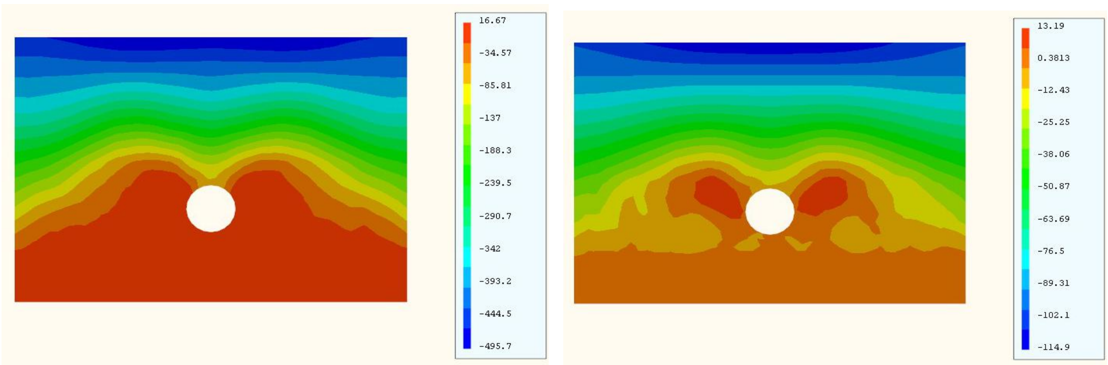

(a) 0.5s (b) 1.0s

Fig. 3 The results of vertical velocity at different time

Analysis of the concrete segment support action under the vibration load

Figure 4 shows the relationship between vertical stress and time, as well as the vertical stress curves of the monitoring points. From the data analysis we can know that the vertical stress of monitoring points 7, 8 and 9 are basically negative. The vertical stress of monitoring point 8 fluctuates between positive and negative, and the positive value is about 100MPa. The curve of monitoring point 7 has the largest fluctuation, it vertical stress is negative which the average value is about 200MPa. The vertical stress of monitoring point 10, 11 and 12 also greatly fluctuate between positive and negative. The vertical stress of measuring points indicated that the U steel protection has improved the passive support strength, but under the condition of vibration load, it is easy to produce stress concentration [6-8]. Under the effect of vibration load, the rigid support as an energy storage body will produce serious stress concentration. Once the damage, it will have a great influence on the deformation of the metro.

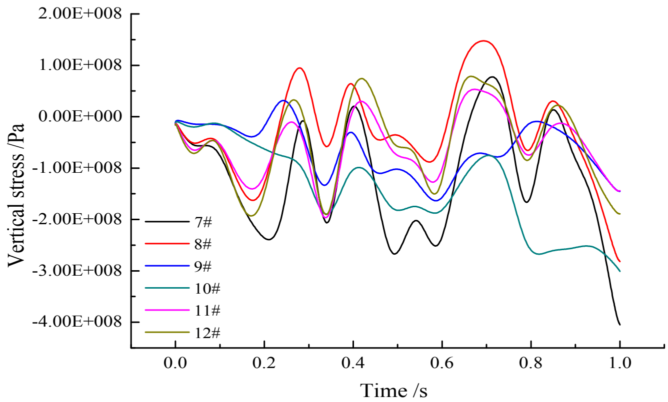

Fig. 4 Vertical stress curves with time

Figure 5 and Figure 6 show the calculation results of vertical velocity and vertical displacement at different times. The results of vertical speed show that the rigid support metro is obviously influenced by vibration load. when t=0.5s, the action of vibration load on metro has enhanced. It has downward action to the metro roof plate, and upward action to the metro bottom plate. Vibration load on the metro both sides has a local concentrate phenomenon, and its distribution is similar to the "bat wing". When t=1s, the effect of vibration load on the metro top roof continue to increase, the distribution of vibration load is similar to the "helmet". Vibration load on both sides of the metro has enhanced, the "bat wing" area is obviously increased. The result of vertical displacement shows that the rock and soil around the metro obviously affected by vibration load, the metro top plate has downward trend, and the metro two sides are squeezed toward inside. The result of metro level profile shows that there are lots of severe displacement deformation area on the metro top and bottom plate, which have a significance influence to the metro deformation failure.

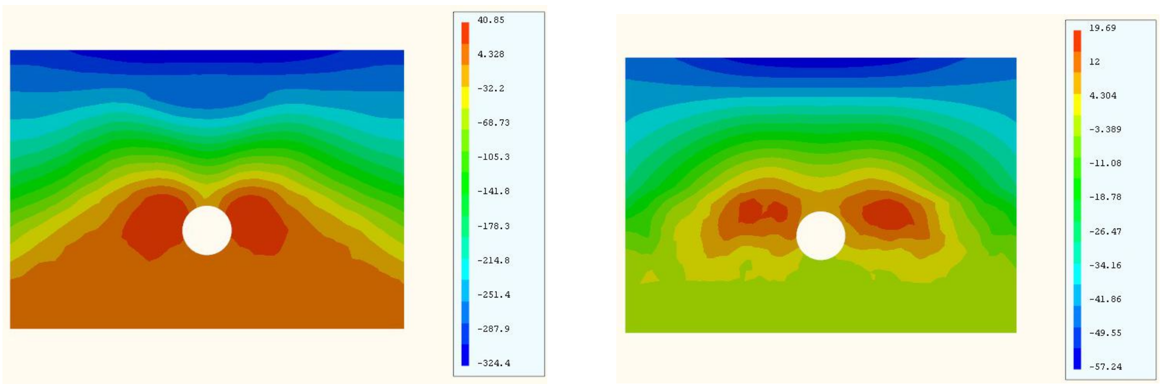

(a) 0.5s (b) 1.0s

Fig.5 vertical velocity results at different times (perpendicular to the metro profile)

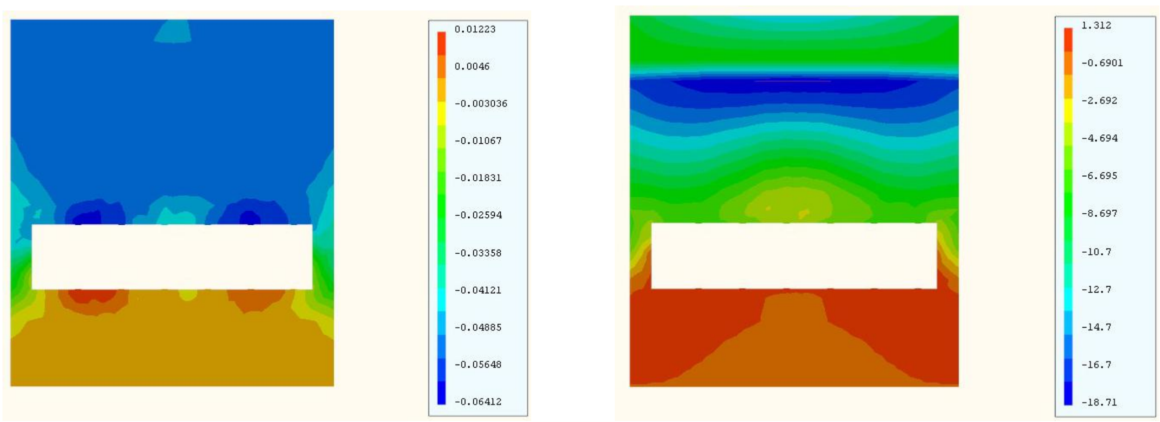

(a) 0.1s (b) 0.5s

Fig. 6 vertical displacement results at different time (parallel to the metro profile)

Stability analysis of underground concrete absorption energy layer

Figure 7 shows the relationship between vertical stress and time, as well as the vertical stress curves of the monitoring points. From the data analysis we can know that the vertical stress of monitoring points 7, 8 and 9 are basically negative. The vertical stress of monitoring point 8,9 fluctuates between positive and negative, and the positive value is about 100MPa. The monitoring point 7 data is negative, its curve fluctuation is the largest and the average value is more than 200MPa. Compared with the monitoring point 7, the value of the monitoring points 8 and 9 greatly reduced, which shows that the concrete energy absorbing layer can effectively reduce the strength of the seismic source wave. The monitoring point 10 data fluctuation is small, monitoring points 11 and 12 data fluctuation is greater, which shows that the seismic wave near the metro bottom plate has weakened [9-11]. Compared with the u-steel support metro, the concrete energy absorbing layer has a larger deformation space, which shows that the deformation of the R-F-R protection metro has obviously reduced, and the metro stability also enhanced[12,13].

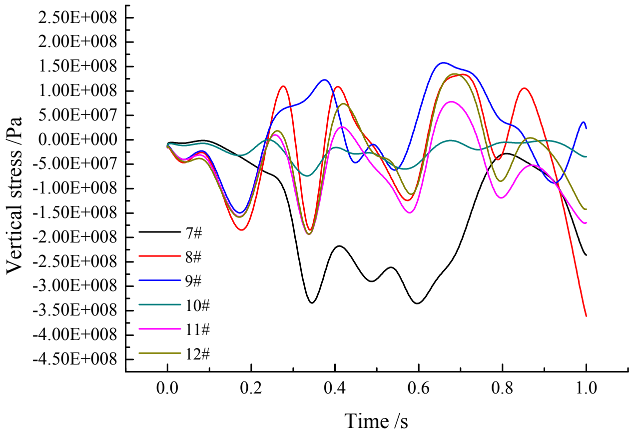

Fig.7 The relationship between vertical stress and time

Figure 8 and figure 9 show the calculation results of vertical speed and vertical displacement at different times. The result of vertical speed shows that the effect of vibration load on the metro has weakened after the concrete energy absorbing layer set up. when t=0.5s, the effect of vibration load on metro has enhanced, the effect of vibration load on the roof is downward, on the bottom plate is upward. When t=0.5s, the vibration load on both sides of the subway is similar to the "bat wing". The distribution area is larger, but the concentrate phenomenon is not obvious. when t=1s, the effect of vibration load continues to increase. The vibration load has wave action to the metro, but the concentrate phenomenon is not obvious, the distribution of vibration load on the metro roof plate is similar to the "helmet", on the metro both sides is similar to the "bat wing". The vertical displacement results shows that the rock and soil around the metro obviously affected by vibration load, the metro top plate has downward trend, and the metro two sides are squeezed toward inside. However, this change has little influence on the metro deformation, this is due to the coordinated deformation of concrete absorbing layer can reduce the surrounding rock deformation. The metro vertical stress and horizontal displacement have obviously reduced, this is due to the concrete energy absorbing layer good coordination deformation performance enable metro can reduce the vibration and vibration intensity, and maintain itself stability [14,15]. Compared with the data of rigid support metro, the vertical force curve volatility decreases and the vertical force of measuring point 8 and 9 also reduced, but the horizontal displacement almost the same. In addition, because the concrete energy absorbing layer has large deformation, so the overall deformation of metro have significantly reduced and there is no obvious deformation concentrated area in the surrounding rock vicinity. This is indicated that the rigid flexible coupling support can fully coordinate deformation, which can reduce the vibration load, improve the impact resistance of deep underground projects, but also conducive to maintaining the stability of the metro.

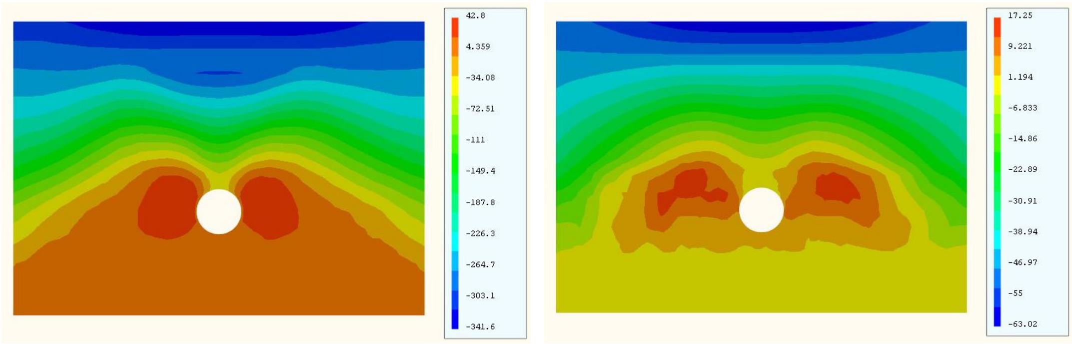

(a) 0.5s (b) 1.0s

Fig.8 Vertical speed results of vertical roadway section

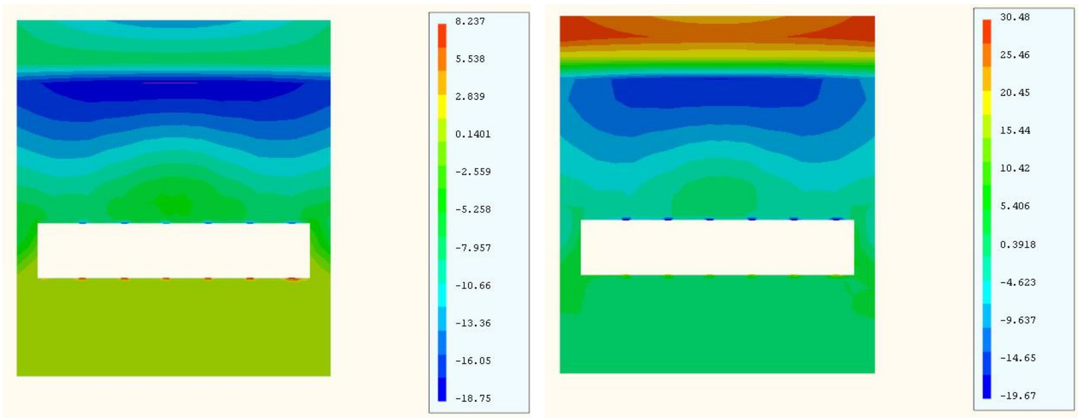

(a) 0.1s (b) 0.5s

Fig.9 Vertical displacement results of parallel roadway section

Conclusions

Based on the continuum mechanics for discrete element calculation method, the shock resistance stability under the action of seismic wave of rigid support and rigid-flexible coupling support deep buried chamber was analyzed. The strengthening and damping action of different protective bodies on the chamber are studied. And the main conclusions are obtained.

Under the condition of vibration load, rigid support as a strong energy storage body can improve the strength of the passive support, but the damage of shock instability becomes easier, and these will lead to the metro extrusion deformation even the overall closure failure;

Concrete energy absorbing layer can effectively the attenuated seismic wave, in the propagation process or near the metro bottom. Under the action of coordinated deformation, the surrounding rock soil deformation tends to be mild and reduced, the stability of the metro enhanced.

Under the action of strong vibration load, the safety of deep buried chamber can be greatly improved by increasing the strength of rigid support and setting up the flexible deformation buffer layer.

ACKNOWLEDGMENTS

This work is supported by the National Natural Science Foundation of China, project number: 51504029. and Beijing Nova program, project number: xx2016041. It is also supported by the sustainable development of the project in Xicheng District City, Beijing science and Technology Commission, project number: SD2014-36. The comments and suggestions from editors and reviewers helping the improvement of the quality of this paper are appreciated very much by the author.

References:

[1] Wang Sijing, Yang Zhifa, Liu Zhuhua. Rock mass stability analysis for underground engineering[M]. Beijing: Science Press, 1984.

[2] Zheng Yingren, Liu Xinghua. Modern nonlinear science and rock mechanic problems[J]. Chinese Journal of Geotechnical Engineering, 1996(1):98-100.

[3] Qian Qihu. Challenges Faced by Underground Projects Construction Safety and Counter Measures[J]. Chinese Journal of Rock Mechanics and Engineering,2012,31(10):1945-1956.

[4] Ren GingWen. Rigid body element method and its application in stability analysis of rock mass[J].Journal of Hohai University, 1995(1):1-7.

[5] Zhiyin Wang, Yunpeng Ling. Sijing Wang. Numerical simulation of the geomechanical processes in rock engineering[J]. International Journal of Rock Mechanics and Mining Sciences,2000,37:439-507.

[6] MS Diederichs, P K Kaiser. Tensile strength and abutment relax-ation as failure control mechanisms in underground excavations[J]. International Journal of Rock Mechanics and Mining sciences,1999,36:69-96.

[7] Lv Qin, Zhang Dingli, Huang Jun. Mechanism of Stratum Deformation and Its Control Practice in Tunneling Urban Subway at Shallow Depth[J]. China Safety Science Journal,2003,13(7):29-34.

[8] Wang Mengshu, Luo Qiong. Construction of shallow buried excavation method in Beijing Metro[J]. Journal of Railway Engineering Society, 1988,(4):107-117.

[9] Sun Jun. Design theory and practice of underground engineering[M]. Shanghai: Shanghai science and Technology Press, 1996:36-42.

[10] Kong Heng, Wang Mengshu, Yao Haibo, etc. Distribution Laws of Stratum Stress With Working Face Excavation in Subway Tunnels[J]. Chinese Journal of Rock Mechanics and Engineering, 2005,24(3):485-489.

[11] P.A. Fotiu, H. Irschik, F. Ziegle. Modal analysis of elastic-plastic plate vibrations by integral equations. Engineering Analysis with Boundary Elements[J].1994, Volume 14, Issue 1:81-97.

[12] Y. Yang, K.P. Kou, C.C. Lam, V.P. Iu. Free vibration analysis of two-dimensional functionally graded coated and undercoated substrate structures. Engineering Analysis with Boundary Elements[J].2015,Volume 60:10-17.

[13] J. R. Shao, S. M. Li, M. B. Liu. Numerical Simulation of Violent Impinging Jet Flows with Improved SPH Method[J]. International Journal of Computational Methods[J].2016, DOI: 10.1142/S0219876216410012.

[14] Liu Daohua, Niu Shixin, Peng Guangsheng, et al. Construction techniques in tackling the collapse in excavating a highway tunnel[J]. Journal of Geological Hazards and Environment Preservation, 2013,24(1):93-98.

[15] Lv Xiangfeng. Excavation Instability Study of Deep Buried Tunnel Consider the Disturbance Action of Earthquake[J]. Tunnel Construction, 2014,34(2):129-133.